혼화재를 사용한 콘크리트의 수화모델

A Hydration Model for Blended Concrete utilizing Secondary Cementitious Powders

노 재 명* 변 근 주** 송 하 원**
Noh, Jea Myoung Keun Joo Byun Ha-Won Song

ABSTRACT

Heat of hydration of concrete under different curing temperatures can be characterized with knowledge of the thermal activity, the heat rate at the reference temperature, and the total heat of hydration of the mixture. The so-called multi-component hydration model incorporates the effect of following variables: cement chemical composition, cement fineness, secondary cementitious powders, mixture proportions, and concrete properties. However, the model does not consider the use of silica fume as a secondary cementitious powder. Therefore, the model that quantifies the heat of hydration due to the use of silica fume is needed. In this thesis, the effects of silica fume on heat of hydration are evaluated and the influence on the heat of hydration are also quantified to be included in the model, so that the analysis using modified multi-component hydration model for silica fume concrete provides more accurate results than normal concrete.

1. Introduction

As admixtures for concrete, various powders such as blast furnace slag, fly ash, silica fume, lime stone powder, expansive agent and so on are used. Blast furnace slag and fly ash have bean especially useful for massive concrete structures because they function as binders and silica fume has bean considered as a main admixture to strengthen concrete. For cement in which several admixtures are used, it is not always rational to treat a whole powder as a single system. In order to apply the effect of silica fume on hydration heat, thermal activity and interactions of each component with silica fume must be investigated and estimated. The objective of this paper is to present the formulation of hydration model for silica fume in concrete. The heat of hydration of concrete under different curing temperatures can be characterized with knowledge of the thermal activity, the heat rate at the reference temperature, and the total heat of hydration in the mixture.

2 Concept of Multi-component Hydration Model

To extend the scope of the model to blended cement, blast furnace slag, fly ash and silica fume are regarded as single components of reaction and incorporated into the model as individual components.

$$H_C = \sum p_i \overline{H}_i$$
$$= p_{C_3A}(\overline{H}_{C_3AET} + \overline{H}_{C_3A}) + p_{C_4AET}(\overline{H}_{C_4AF} + \overline{H}_{C_4AF}) + p_{C_2S}\overline{H}_{C_2S} + p_{C_2S}\overline{H}_{C_2S} + p_{SG}\overline{H}_{SG} + p_{FA}\overline{H}_{FA} + p_{SF}\overline{H}_{SF} \quad (1)$$

$$H = CH_C \quad (2)$$

The hydration heat rates of blast furnace slag, fly ash and silica fume are described by two material functions. Therefore, the hydration heat rate of each component is generally expressed, with interdependency among the reactions, as follows,

$$\overline{H}_i = \beta_i \gamma \mu \lambda s_i H_{i,T_r}(Q_i) \exp\left[-\frac{E_i(\overline{Q}_i)}{R}\left(\frac{1}{T} - \frac{1}{T_o}\right)\right] \quad (3)$$

$$Q_i = \int \overline{H}_i dt \quad (4)$$

* 정회원, 한국전력공사 전력연구원 연구원
** 정회원, 연세대학교 사회환경시스템공학부 교수

3. Multi-component Hydration Model utilizing Use of Silica Fume

To quantificate the heat of hydration, the result of Ma et al. (1994) is analyzed by using Suzuki model. The heat rate in terms of elapsed time is converted to one in terms of accumulated heat (Fig 1)

The total heat generation ($Q_{i,\infty}$) per unit weight, which corresponds to 100% reaction, can be derived from qualitative observations of reactions besides analytic trials. The total heat generation of silica fume in reference heat generation rate was set as a temporal value. From Table 1, total heat generation of silica fume in phases of cement can be taken 185 kcal/kg.

Generally, reaction per unit mass proceeds faster with finer particles. Reference heat rate is changed according to powder fineness and s_i represents the change of referential heat rate.

$$s_i = S_i / S_{ft} \qquad (5)$$

Fig 2 shows Arrhennious plots of OPC, fly ash cement, GGBS cement and silica fume cement. The gradients of the trend lines mean thermal activities of each cement.

Through heat rate of silica fume blended cements compares with other cement, thermal activity of silica fume can be estimated. Therefore, the thermal activity of silica fume can assumed -1500K with comparing the existing thermal activity assumed by Maekawa, K., Kishi, T., and Chaube, R., (Fig 5)

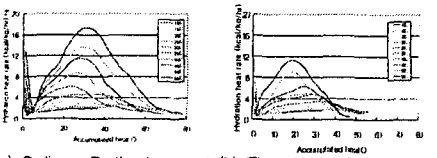

(a) Ordinary Portland cement (b) Fly ash blended cement

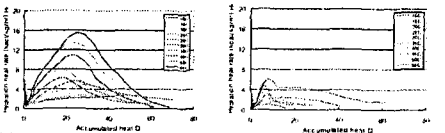

(c) silica fume blended cement (d) GGBS blended cement

Fig 1 Heat rate of ordinary Portland cement in terms of accumulated heat

Table 1 Enthalpy of complete hydration for hases of cement (Bentz, Waller, and de Larrard, 1998)

Phase	Enthalpy(kcal/kg)
Tricalcium silicate	123.46
Dicalcium silicate	62.57
Tricalcium aluminate	273.19
Tetracalcium aluminoferrite	173.13
Silica fume	186.24

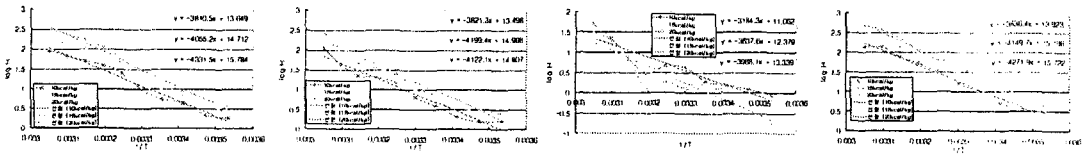

(a) OPC (b) fly ash cement (c) GGBS cement (d) silica fume cement

Fig 2 Arrhennious plots

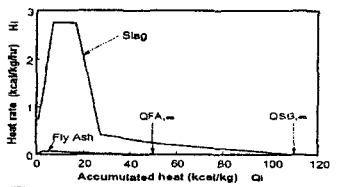

Fig 3 Reference heat generation rate of fly ash and slag (Maekawa, et al. 1999)

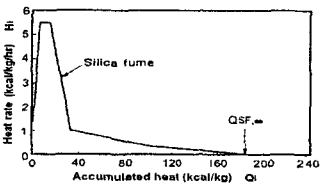

Fig 4 Reference heat generation rate of silica fume

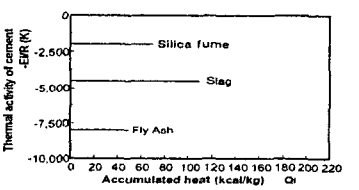

Fig 5 Thermal activities of each secondary cementitious powders

4. Verification and Analysis of Proposed Multi-component Hydration Model

4.1 Early-age strength analysis

The relation between them should be formulated according to the mix proportion and used powder materials. The compressive strength is expressed in terms of the total differential equations as

$$f_{c'} = \int df_{c'} \qquad df_{c'} = 25dQ_{3s} + 40dQ_{2s} + 27dQ_{SG} + 30dQ_{FA} + 45dQ_{SF}$$
$$dQ_i = \frac{p_i}{W_{total}} d\phi_i \qquad \phi_i = \frac{Q_i}{Q_{i,\infty}} \qquad (6)$$

Fig 6 shows the analytical results in concrete utilizing secondary cementitious powders with respect to the curing time within a day.

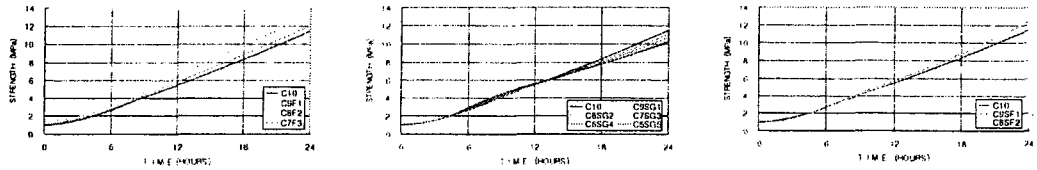

(a) fly ash concrete (b) GGBS concrete (c) silica fume concrete

Fig 6 Calculated strength variation in terms of time

4.2 Temperature Analysis

4.2.1 Heat rate analysis for use of secondary cementitious powders

In other to show the change of heat rate due to the replacement ratio of fly ash, replacement ratio of fly ash is increased from 0 to 40% with 10% replacement step. In other to show the change of heat rate due to the replacement ratio of GGBS, replacement ratio of GGBS is increased from 0 to 60% with 10% replacement step. In other to show the change of heat rate due to the replacement ratio of silica fume, replacement ratio of silica fume is increased from 0 to 30% with 10% replacement step. From Fig 3, the peak heat rate does not change any more above 20% of silica fume replacement. The reason why no change of heat rate occurs is the rapid consumption of calcium hydroxide while silica fume reacts.

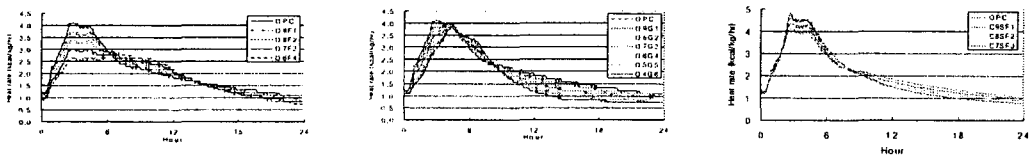

(a) fly ash concrete (b) GGBS concrete (c) silica fume concrete

Fig 7 Calculated heat rates of fly ash concrete in multi-component model

4.2.2 Temperature analysis for the use of silica fume

The experiment results, conducted by Highway research center of Korea highway corporation, was compared with the analysis using proposed hydration model. Fig 8(a) shows the shape of specimen(80cm×110cm×90cm). Fig 8(b) shows generated meshes for temperature analysis. In order to compare analysis results with experiments, the temperature at the center point is analyzed.

The properties of the cement, used in the experiment, are as described in table 2. The chemical contents of silica fume and physical properties are in table 3.

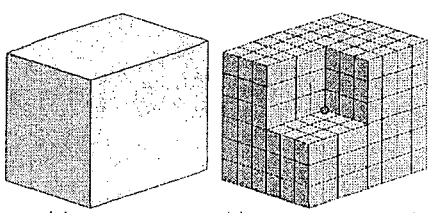

(a) specimen (b) mesh plot for analysis

Fig 8 Shape of specimen

Table 2 Properties of ordinary Portland cement in the experiment

Chemical contents (wt, %)							Physical properties	
SiO_2	Al_2O_3	Fe_2O_3	CaO	MgO	SO_3	Ignition loss	Blaine value (kg/m²)	specific gravity
21.95	6.59	2.81	60.12	3.32	2.11	2.58	3.117	3.15

Table 3 Properties of silica fume

Chemical contents (wt, %)										Surface area (m²/g)	Specific gravity	Unit weight (kg/m³)	Blaine value (μm)
SiO_2	Fe_2O_3	Al_2O_3	CaO	MgO	Na_2O	K_2O	C	S	L.O.I				
94.0	0.8	0.3	0.3	0.4	0.2	0.8	1.0	0.2	2.8	18-20	2.2	250-300	0.1-0.2

Table 4 is the mix proportion of silica fume concrete and normal concrete.

Table 4 Mix proportions of concrete

design strength (kg/cm²)	max diameter of aggregate (Ψ,mm)	W (kg)	C (%)	W/C (%)	S/a (%)	S (kg)	silica fume (kg)
700	19	160	552	29	40	668	82.6
400	25	195	488	40	40	663	

Temperature analysis result of analysis is plotted in Fig 9 and 10. The analyzed temperature shows more similar with experiments than temperature analysis of normal concrete in Fig 6.19.

In Fig 11, the wall structure to compare experiment and analysis is shown. In other to verify adaptability of proposed model, virtual analysis is conducted. In Fig 12, the analysis results of silica fume concrete are plotted. Temperatures, at the center and the surface of the wall, are plotted. In 80cm thick wall, the peak temperature is increased to 70℃ while, the peak is increased 60℃ in 60cm wall. In table 5, virtual mix proportion and thermal properties of each material are shown.

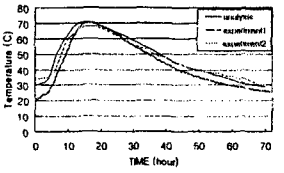

Fig 9 Temperature analysis of silica fume concrete

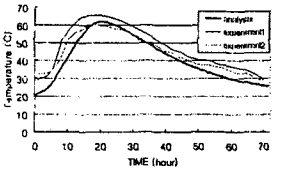

Fig 10 Temperature analysis of normal concrete

Table 5 Mix proportions of silica fume concrete for analysis

Mix	unit weight (kg/m^3)				
	cement	silica fume	water	fine aggregate	coarse aggregate
opc	357	-	178	882	927
sf5	339.15	17.85	178	882	927
sf10	32.13	35.7	178	882	927
sf15	303.45	53.55	178	882	927

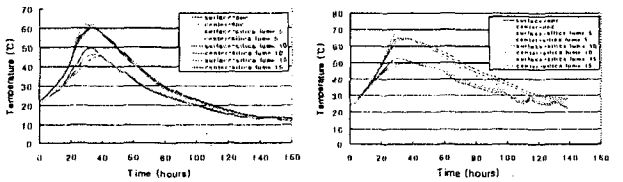

(a) 80cm thick massive wall (b) 60cm thick massive wall

Fig 12 Temperature analysis results

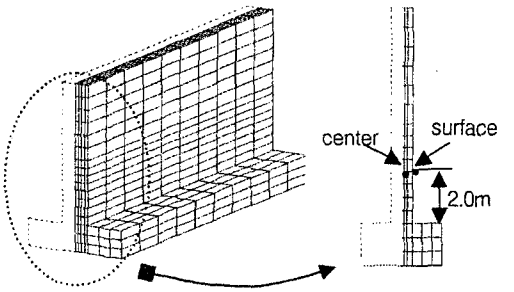

Fig 11 Finite element mesh of wall structure and the point to compare

5. Conclusion

The effect of initial temperature on the ultimate temperature rise is discussed by considering heat generation related to reaction before casting. The reactions of blast furnace slag, fly ash and silica fume are modeled to be dependent on the amount of calcium hydroxide produced by cement hydration. Using proposed heat generation rate, temperature analysis of silica fume concrete can be performed. The applicability of the proposed model was verified by analyzing the results of existing temperature tests. The analysis using proposed model in silica fume concrete provides more accurate results than normal concrete. Therefore, temperature prediction in silica fume concrete is available to engineer using modified multi-component hydration model.

References

1. ACI Committee 234, (1996), "Guide for the use of silica fume in concrete", America Concrete Institute.
2. Bentz, D.P., Waller, V., and de Larrard, F., (1998), "Prediction of adiabatic temperature rise in conventional and high-performance concretes using a 3-D microstructural model", Cement and Concrete Research, Vol. 28, 285-297.
3. Ulm, F.J., and Coussy, O., (1998), "Couplings in early-age concrete: from material modeling to structural design", Int. J. Solids Structures, Vol. 35, 4295-4311.
4. Maekawa, K., Kishi, T., and Chaube, R., (1999), Modeling of concrete performance, E & FN SPON.
5. Ma, W., Sample, D., Martin, R., and Brown, P. W., (1994), "Calorimetric study of cement blends containing fly ash, silica fume, and slag at elevated temperatures", Cement, Concrete, and Aggregates, Vol. 16, 93-99.
6. Suzuki, Y., Harada, Y., Maekawa K., and Tsuji, Y., (1990), "Quantification of heat of hydration generation process of cement in concrete", Concrete Library of JSCE, No. 16, 111-123.
7. 岸 利治, 鈴木 康範, 前川 宏一, (1990), "水和發熱モデルにおけるフライアッシュセメントの材料特性値のモデル化", 土木學會第45回年次學術發表會, V-176.
8. 안태송, 이병덕, 유환구, (1995), 특수콘크리트의 실용화연구, 한국도로공사 도로연구소.